

Grating Interferometers for Efficient Generation of Large Area Grating Structures via Laser Ablation

Jozsef BEKESI, Jörg MEINERTZ, Jürgen IHLEMANN and Peter SIMON

*Laser-Laboratorium Göttingen e.V., Hans-Adolf-Krebs-Weg 1, 37077 Göttingen, Germany
E-mail: jbekesi@llg.gwdg.de*

A two-grating interferometer setup is described for fabricating large area grating structures via laser ablation with UV femtosecond pulses. Phase grating pairs on fused silica substrates with high damage threshold and diffraction efficiency were illuminated with non-collimated (convergent) laser beams to generate a periodic intensity distribution with high energy density and high contrast on the sample surface. Large line numbers without phase distortions were reached by applying cylindrical focusing perpendicular to the grating lines. Scanning the illuminating laser beam in the direction parallel to the grooves enabled the fabrication of cm-scale grating sizes with multiple shot ablation, while keeping the whole line structure in phase. Complex patterns are possible by applying multiple exposures. Experimental results demonstrating the capability of the method to generate laser ablated grating structures with submicron periods down to ~ 300 nm are presented.

Keywords: Laser nanofabrication, laser-induced gratings, surface texturing, submicron structuring, phase masks, grating interferometers

1. Introduction

It is a general trend to reduce the size of optomechanical components, often having feature sizes below one micron. Also, the fabrication of 2- and 3-dimensional periodic structures, specifically the creation of photonic crystals has attracted tremendous interest in recent years. All these applications are generating a growing demand for the development of fast, low-cost, and flexible fabrication technologies. Laser direct processing via surface ablation offers exactly these properties, thus representing a great potential for such applications in science and technology.

Laser ablation is a well established method for micro structuring of many materials like e.g. polymers, glasses, and ceramics. Applying ultrashort pulses (pico- or femtosecond pulse duration) reduces the so-called heat-affected zone [1], thus providing an even better precision of the ablation process. This opens the way towards high precision processing of more challenging materials like metals. Combining the short pulse duration with a UV wavelength (248 nm) provides a lateral resolution well below $0.5 \mu\text{m}$ [2,3].

In industrial applications of laser micro-fabrication, beside the spatial resolution limit the processing speed is a further fundamental issue. There are several well known optical schemes for laser processing: e.g. focus scanning, mask imaging or different interference techniques. All these techniques have their advantages and drawbacks for a given application. Focus scanning offers the capability of creating arbitrary structures, thus providing a great flexibility in fabricating a variety of structures. However, the processing speed is strongly limited in case of large sample areas (sequential processing). In contrast, mask projection allows the treatment of an extended sample area at the same time (parallel processing).

In particular, for the fabrication of periodic nanostructures, interference techniques are ideally suited. In

such schemes the incoming laser beam is split into partial beams which are then recombined on the sample surface. In case of temporal and spatial overlap of the beams, the resulting interference pattern is converted into the desired surface texture. Following the approach of combining interference techniques with mask projection, gratings with periods of ~ 400 nm have been fabricated on different metal and semiconductor samples [4-6]. An extension of this method using the interference of multiple beams can be the key to the fabrication of complex 2- and 3-dimensional structures, specifically for the creation of photonic crystals [3]. The drawback of this technique is the limited size of the generated image on the sample surface caused by the difficulty in realizing distortion free imaging in the UV, especially by using ultrashort laser pulses. Therefore, fabrication of large area grating structures by laser ablation remains a challenging task, especially if the whole area must be patterned with a high definition submicron-period line structure in perfect registry.

In classical holography tremendous efforts have been made to develop a technique for fabricating large area gratings without optical distortions. The main problem was the low coherence of the applied sources. To solve this problem achromatic holographic arrangements have been introduced allowing the generation of high quality, large and distortion free illumination patterns with very high contrast even for illuminating sources of poor coherence properties. One such arrangement is based on the principle of grating interferometers. These devices have been extensively discussed in the literature for applications in holographic lithography. The possibility of fabricating large area gratings even with white light sources has been demonstrated [7-10].

The main idea discussed in the present publication is to adopt the above technique for laser ablation. A fundamental challenge is to insure a sufficiently high energy density on the sample surface necessary to exceed the ablation thresh-

old of most materials. In the early applications of grating interferometers for the generation of large gratings, the need to reach high energy densities was not a limiting factor because only photo resist irradiation was required for subsequent wet etching.

To overcome these difficulties we propose a focusing scheme instead of the earlier used magnifying layouts to reduce the beam size on the sample to reach the necessary fluence for ablation. The detailed description of such an arrangement and the results are given in the following sections.

2. Two-grating Interferometers

A two-grating interferometer in its basic form consists of two gratings placed parallel to each other. The light illuminating the first grating will be diffracted, forming several beams. These beams, again, will all be diffracted by the second grating. If some of the beams overlap in a third plane, fringes will be formed with a characteristic intensity distribution (depending on e.g. the number of intersecting beams and their relative intensity). For the generation of a sinusoidal intensity distribution only two beams are required and all the others must be blocked. Such a simple arrangement is shown in Fig. 1. The line period of the first grating (G_1) is p_1 , that of the second grating (G_2) is p_2 . They are placed parallel to each other so that also the grating lines are aligned to be exactly parallel. The arbitrary separation of the gratings is z_1 . The plane of fringe formation is located in a distance of z_2 behind G_2 . The two beams diffracted at G_1 into the ± 1 st orders hit the second grating, all other beams are blocked. After diffraction on G_2 again all beams are blocked except the two indicated in the figure: the $+1$ st order beam emerging from G_1 diffracted into the -1 st order at G_2 and the -1 st order beam emerging from G_1 diffracted into the $+1$ st order at G_2 . If $p_1 = 2p_2$ then the above mentioned beams will completely overlap in plane P, located at a distance $z_2 = z_1$ behind G_2 . The interference pattern in plane P will have the same period as G_2 .

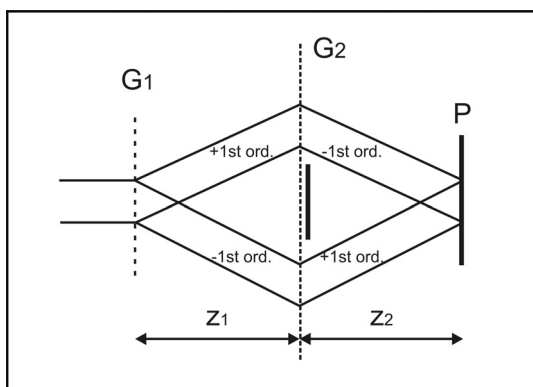


Fig. 1 Two-grating interferometer with collimated beams.

This special type of two-grating interferometer was discussed by Hershey and Leith [8]. They have discussed theoretically and also demonstrated experimentally the very special feature of this setup, that a high definition, unit-contrast, straight fringe pattern will be formed, even if the illuminating beam has neither spatial nor temporal coherence. Although these properties are only fulfilled if the

gratings are perfectly formed and aligned, the tolerances are greatly relaxed for illuminating sources with partially coherent sources. Yen et al. showed that large area, spatially coherent gratings with 100 nm period can be generated on a photoresist by illuminating it with an ArF excimer laser with relatively poor coherence [9].

Such an arrangement could in principle be used for laser ablation, if the required energy density for ablation can be reached in plane P. This requires a modification of the setup. The energy density on the sample surface (plane P) should be significantly higher than on the gratings, thus allowing to reach the ablation threshold of most materials without damaging the gratings themselves. A possible solution can be to insert a focusing element in front of the grating pair. To keep the distance between the gratings and also the necessary grating size reasonably small, relatively short focal length lenses should be used. Unfortunately, as already discussed in [9], for non-collimated beams the sensitivity of the whole arrangement to slight misalignments rapidly increases, thus imposing strong limitations on the practicability of the scheme.

To avoid the above limitations we propose to use cylindrical focusing. Using a focusing in the direction of the grating lines while keeping the beam collimated in the diffraction plane of the gratings has several advantages. First, in the line focus the energy density is high enough to ablate most of the materials. Second, in the plane of diffraction (perpendicular to the grating lines) the beam remains collimated, keeping any distortions originating from a possible imperfect alignment on a negligibly low level. As a result, high quality grating structures with very large line numbers can be generated. Scanning the beam in a direction parallel to the grating lines will always illuminate a different stripe on the sample surface while keeping the whole structure perfectly in phase, thus enabling the fabrication of large area grating structures.

3. Experiments

For the experiments we used a femtosecond UV laser system delivering ~ 500 fs pulses at 248 nm [11]. The energy of the pulses was controlled by a variable attenuator. To increase the spatial uniformity of the beam a special beam homogenization method was applied, which was optimized for femtosecond UV systems (described in [12]). Grating pairs with periods of 950 nm/475 nm and 662 nm/331 nm for G_1/G_2 have been tested. In order to minimize energy losses (increase the overall transmission of the grating interferometer in the "useful" diffraction orders shown in Fig.1), high efficiency fused silica phase grating pairs were used, optimized for TE polarized 248 nm irradiation (Ibsen Photonics, Denmark). A $\lambda/2$ plate was used to adjust the polarization of the laser beam relative to the grating grooves. The overall transmission efficiency for the "useful" ± 1 st order beams was 33% for the grating interferometer with the larger period and slightly over 50% for the one with the finer grooves, respectively. The differences in the overall transmission efficiency can be explained by the different grating periods and by the design of the grating masks. The planes of the gratings were adjusted to be parallel to each other and to be perpendicular to the incoming beam. The grating lines were also adjusted

to be exactly parallel to each other. The samples were mounted on an xyz positioning system which was also adjusted to be perpendicular to the laser beam. To check the adjustment of the grating pairs an online monitoring system was built and mounted on the xyz positioning system. This system allowed us to monitor the created intensity pattern in the sample plane. For magnification a high numerical aperture UV objective was used (Zeiss Ultrafluar) in combination with a UV sensitive CCD camera. The resolution of the monitoring system was 45.5 pixel/ μm .

The lens for cylindrical focusing had a focal length of $f = 60$ mm for the 475 nm setup and $f = 200$ mm for the 331 nm setup, respectively. The relatively large distance between G_2 and P (e.g. 40 mm for the 331 nm setup) also ensures to minimize contamination by debris, no observable contamination of G_2 occurred. In both setups the cylindrical lens was mounted on a rotational stage which was mounted on a xyz positioning unit. The focal line of the lens was aligned to be exactly perpendicular to the grating lines. By translating the cylindrical lens along the optical axis the energy density on the sample could be varied. In most cases the focal plane of the lens was behind plane P.

4. Results

To demonstrate the capability of the setup for ablation, different materials have been tested. In Fig. 2 an SEM (Scanning Electron Microscope) picture of a 125 μm thick PI (polyimide) sample (Goodfellow) is shown. On the sample an area of 3.7 mm x 3.6 mm was irradiated with 350 pulses, scanning a beam stripe of 175 μm times 3.6 mm over the sample by moving the cylindrical lens at constant velocity perpendicular to the plane of diffraction (along the grating lines). The energy carried in the two 1st order beams was measured to be 115 μJ . Thus we can conclude that the average energy density in the scanning beam was ~ 20 mJ/cm², and each position of the sample was on average irradiated by 16 pulses (overlapping factor: 1/16), at a repetition rate of 6 Hz. Assuming unit contrast of the sinusoidal grating structures the peak fluence is twice as high as the average energy density.

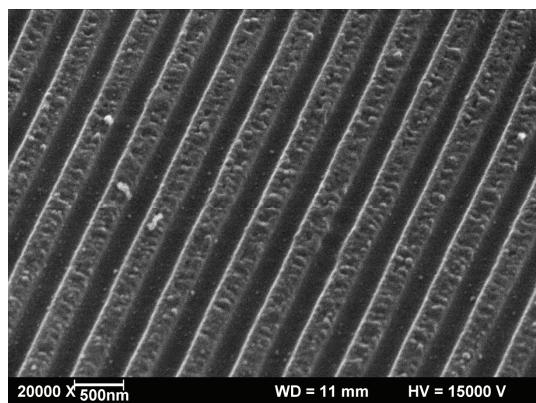


Fig. 2 Linear grating structure on PI film with a period of 475 nm.

We also tested the grating setup which is designed to create periods of 331 nm. In that case, the area of the generated grating structure was 5 mm x 13 mm. This area was

illuminated with a total of 910 laser pulses. In this case, the size of the scanning beam was 665 μm x 13 mm. The average energy density on the sample surface was ~ 15 mJ/cm² (120 pulses/position, 6 Hz repetition rate). An SEM picture of the structure is shown in Fig. 3.

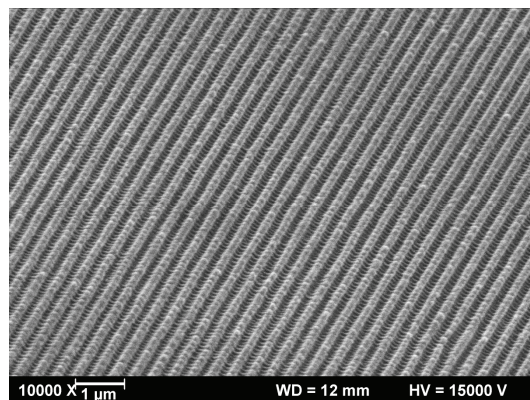


Fig. 3 Linear grating structure on PI film with a period of 331 nm.

Similar structures were also generated on polished steel samples (4 mm thick tool-steel (No 1.2842) plates). The grating structure in Fig. 4 was generated over an area of 3.7 mm x 3.6 mm with 1660 pulses (scanning beam size: 50 μm x 3.6 mm, 22 pulses/position, 6 Hz repetition rate). The calculated average energy density on the sample surface was 80 mJ/cm².

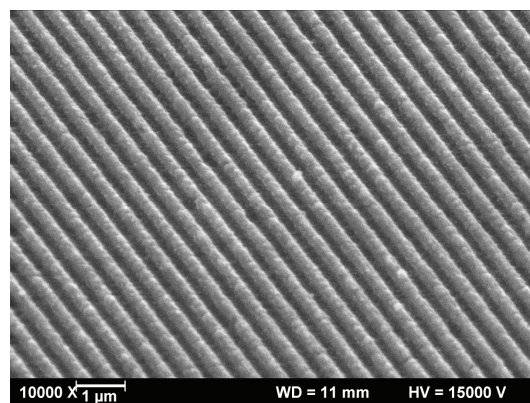


Fig. 4 Linear grating structure on polished steel plate with a period of 475 nm.

By applying multiple illumination and rotating the sample between the illuminating phases, it is possible to generate more complicated patterns on the samples. In the simplest case, a periodic dot pattern can be ablated onto the sample upon rotating it by 90°. Such a crossed grating structure is shown in Fig. 5. This pattern was generated with the same laser parameters like the grating structure in Fig. 2, in two subsequent steps.

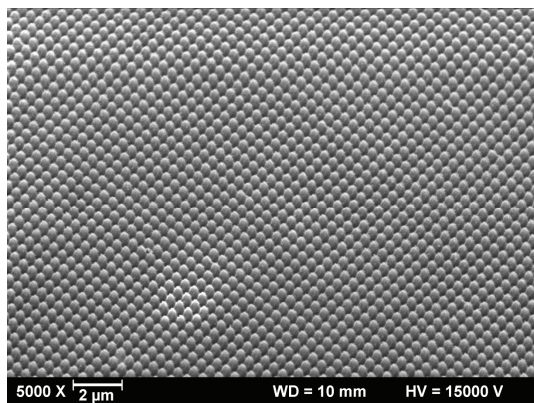


Fig. 5 Crossed grating structure on PI film with a period of 475 nm.

Although the cross section of the ablated structures was not directly characterized, theoretical considerations predict a sinusoidal shape. The exact form depends on the material and the applied fluence. The SEM pictures indicate structure depths on the order of half the period or more.

5. Conclusion

A two-grating interferometer setup has been introduced for producing large area grating structures via laser ablation. The applied cylindrical focusing in the direction of the grating lines allowed us to increase the energy density exceeding the ablation threshold of materials like polymers or metals on the sample surface without damaging the fused silica phase masks. Scanning with the illuminating laser beam in the direction parallel to the grating lines enabled the fabrication of cm-scale grating sizes with multiple shot ablation, while keeping the whole line structure in phase. Generation of complex patterns is possible by applying multiple exposures. Ablated grating structures with periods down to 331 nm are presented. The setup is also applicable for laser sources with poor coherence properties.

6. Acknowledgement

Financial support from the BMWi of Germany (grant no. 16IN0393) is gratefully acknowledged.

References

- [1] E. Matthias, M. Reichling, J. Siegel, O.W. Käding, S. Petzoldt, H. Skurk, P. Bizenberger, E. Neske: *Appl. Phys. A* 58, (1994) 129.
- [2] J. Bekesi, J.-H. Klein-Wiele, P. Simon: *Appl. Phys. A* 76, (2003) 355.
- [3] J.-H. Klein-Wiele, P. Simon: *Appl. Phys. Lett.* 83, (2003) 4707.
- [4] P. Simon, J. Ihlemann: *Appl. Phys. A* 63, (1996) 505.
- [5] K. Chen, J. Ihlemann, P. Simon, I. Baumann, W. Sohler: *Appl. Phys. A* 65, (1997) 517.
- [6] F. Beinhorn, J. Ihlemann, P. Simon, G. Marowsky, B. Maisenhölder, J. Edlinger, D. Neuschäfer, D. Anselmetti: *Appl. Surf. Sci.* 138–139, (1999) 107.
- [7] B.J. Chang, R. Alferness, and E.N. Leith: *Appl. Opt.*, 14, (1974) 1592.

- [8] R.R. Hershey, and E.N. Leith: *Appl. Opt.*, 29, (1990) 937.
- [9] A. Yen, E.H. Anderson, R.A. Ghanbari, M.L. Schattenburg, and H.I. Smith: *Appl. Opt.*, 31, (1992) 4540.
- [10] I.N. Ross, C.J. Hooker, and P. Dombi: *Appl. Opt.*, 40, (2001) 6153.
- [11] J. Bekesi, S. Szatmári, P. Simon, G. Marowsky: *Appl. Phys. B* 75, (2002) 521.
- [12] P. Simon, and J.-H. Klein-Wiele: DE Patent 10249532 (2002).

(Received: April 24, 2007, Accepted: October 11, 2007)